

$L_{2,3}M_{4,5}M_{4,5}$ x-ray-excited Auger-electron spectra of Ag

G. G. Kleiman, S. G. C. de Castro, and R. Landers

Instituto de Física "Gleb Wataghin," Universidade Estadual de Campinas, 13081-970 Campinas, São Paulo, Brazil

(Received 8 June 1993; revised manuscript received 13 September 1993)

We have investigated the $L_{2,3}M_{4,5}M_{4,5}$ Auger spectra of Ag excited with bremsstrahlung. The main experimental spectra are in good agreement with atomic-multiplet-structure calculations in which the initial state is treated in jj coupling and the final state in the intermediate coupling scheme. Anomalous loss structures appear at lower energies than those of the main spectra. These losses appear to be atomic in origin and are not manifest in the corresponding spectra of In, Sn, and Sb. We demonstrate that these losses are consistent with a model of d -band spectator vacancy shake-up satellites. Coster-Kronig processes present in Cu appear to be absent here.

I. INTRODUCTION

X-ray-excited Auger-electron spectra (XAES) of purely core-level transitions (i.e., ijk transitions) in noble and transition metals and their alloys are often investigated because of the localized nature of the core levels. For example, since our current understanding of Auger energies is based upon the local character of the final-state holes, predictions of energies^{1,2} should be compared to the results of measurements of ijk spectra. Furthermore, Auger energy shifts in alloys, which complement x-ray photoelectron spectroscopy (XPS) binding-energy shifts,^{3,4} should be measured from ijk spectra.⁵ Finally, comparison of experimental and atomic theoretical core-level spectra permits both critical evaluation of the atomic theories and identification of solid-state effects.

Although XAES ijk spectra do not yield the direct valence-band information often embodied in spectra of transitions involving final-state d -band holes (i.e., iVV transitions), their energies can furnish considerable information regarding the nature of the valence states.⁶ For example, measured ijk Auger peak energy shifts can provide information regarding relative Fermi energies^{3,7} and Auger shifts can be combined with XPS shifts to elucidate electronic-structure changes induced by alloying.^{8,9} Moreover, Auger parameters calculated from ijk energies can be analyzed according to fundamental considerations to determine the screening contribution from valence electrons.¹⁰⁻¹⁴

Usually, however, such analyses are hampered because of the considerable breadth of the ijk spectra which results from the superposition of contributions from various terms.^{15,16} In recent work,^{5,10-14} we demonstrated that, in contrast to the broad spectra of the $L_{2,3}M_{2,3}M_{2,3}$ transitions in the $3d$ series,¹⁵ and the $N_{6,7}O_{4,5}O_{4,5}$ transitions in Tl, Pb, and Bi,¹⁶ the high-energy LMM and LMN spectra in the $4d$ metals are narrow and simple in form, although weak.^{10,13,14} These spectra were analyzed to infer a number of results regarding valence as well as core states.^{5,10-14}

In particular, in a recent paper,¹⁰ which we denote as I, we reported the experimental $L_2M_{4,5}M_{4,5}$ and $L_3M_{4,5}M_{4,5}$ Auger spectra of In, Sn, and Sb and com-

pared them with the results of atomic calculations using the jj intermediate coupling scheme¹⁶ for the initial and final states. As in other treatments,¹⁵⁻¹⁷ satisfactory agreement between theory and experiment was reached when the problem was considered as atomic in nature.¹⁰

Since the $4d$ bands are full in the metals considered in I, it is interesting to investigate the form of the $L_{2,3}M_{4,5}M_{4,5}$ spectra in metals for which there are holes in the initial-state d band. In this paper, we report the results of such a study for Ag, which is intermediate between the $4d$ transition and sp metals because of the small number of d -band holes produced by $s-d$ hybridization. The form of the main spectra agrees with the results of jj intermediate coupling calculations, as in I. There appear, however, anomalous loss structures at lower kinetic energies whose origins seem different from any yet reported. We identify them as arising from d -band spectator vacancy satellites and show that this model is consistent with all the aspects of the data. Coster-Kronig processes present in Cu are apparently absent here.

In Sec. II, we report the experimental results, in Sec. III, we discuss them and, in Sec. IV, we present the conclusions. Throughout, we draw freely on theoretical results reported in I.

II. EXPERIMENTAL RESULTS

The sample preparation and experimental procedures are reported elsewhere.⁵⁻¹⁴ In Figs. 1 and 2, we present, respectively, the $L_3M_{4,5}M_{4,5}$ and $L_2M_{4,5}M_{4,5}$ Ag Auger spectra excited with bremsstrahlung.^{18,19} The top portion of each figure displays the raw spectral data (dots) as well as the corresponding background (solid curve) calculated as a constant fraction of the experimental intensity integrated to higher kinetic energy than that considered.²⁰ In the bottom portion of each figure, we also present the corresponding data (dots) with the background subtracted for comparison with theoretical spectra. In order to underscore the similarity of the loss structures below the main peaks in both the $L_3M_{4,5}M_{4,5}$ and $L_2M_{4,5}M_{4,5}$ spectra, which we discuss below, the raw data has been plotted such that, in each figure, the difference between the maximum intensity and that corre-

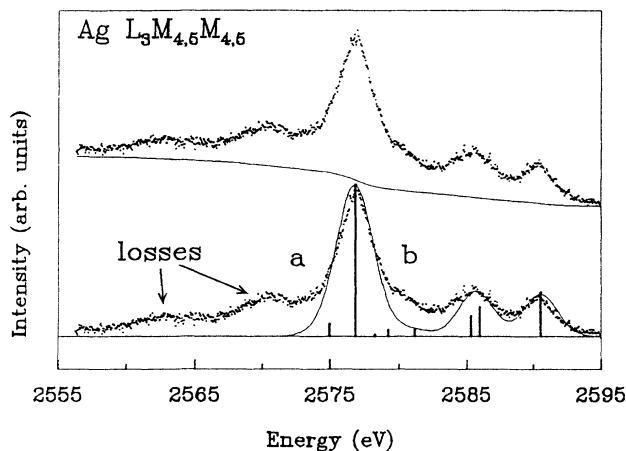


FIG. 1. The $L_3M_{4,5}M_{4,5}$ Auger spectrum of Ag as a function of kinetic energy. The data are represented by dots. The raw data are presented in the upper portion, together with the background calculated from integrating the experimental spectrum to higher energies. In the bottom portion is the background subtracted spectrum. The bar diagrams represent the corresponding intermediate (IC) coupling intensities from Table I. The solid line represents the atomic spectrum generated by Gaussian broadening of width 3.2 eV.

sponding to the lowest energy considered is the same. For future reference, we should point out that the ratio between the areas of the background subtracted L_3 and L_2 spectra is around 2.2, which is quite close to the statistical ratio of 2, considering the uncertainties involved in measuring the areas and defining the background.

All of the spectra exhibit several peaks to the right of the main peak whose relative energies agree with final-state term splittings calculated in the intermediate coupling (IC) scheme.²¹ As pointed out in I, the LS coupling

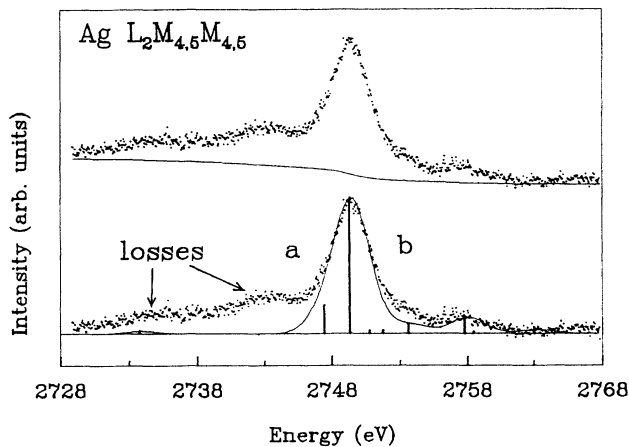


FIG. 2. The $L_2M_{4,5}M_{4,5}$ Auger spectrum of Ag as a function of kinetic energy. The same conventions as in Fig. 1 are used here. The scale used in displaying the data is such that the difference between the raw data intensities at the minimum energy and at the main peak is the same as in Fig. 1. The Gaussian broadening is of width 3.1 eV.

scheme, whose results we do not display, is inadequate in these cases. The results of the calculations of the multiplet energies treating the final state in the IC coupling scheme are presented in Table I. The atomic Coulomb integrals used were those of Mann²² and the spin-orbit parameter used in the IC calculations was 2.40 eV, as derived from the experimental M_4 - M_5 XPS splittings.²³

The transition rates were also calculated in the intermediate coupling approximation using the radial integral calculated by McGuire.²⁴ The results for the $L_3M_{4,5}M_{4,5}$ and $L_2M_{4,5}M_{4,5}$ IC transition rates relative to that of the most intense term are shown in the fourth and fifth columns of Table I. For the jj IC calculations, the eigenvector mixing coefficients²¹ corresponding to the entries in Table I are those in Table II and the equations used¹⁶ are given in the Appendix of I.

The results of these atomic calculations are represented as bars in the bottom portions of Figs. 1 and 2: their separations correspond to the calculated multiplet splittings and their heights reflect the calculated relative intensities in the jj IC approximation. In order to better demonstrate the agreement between the experimental and theoretical atomic spectra, we also present the fittings of the data for energies at and above the main peak to an envelope function (solid curve) generated from the multiplet structure calculations. To form this envelope, all the components were represented by Gaussians whose widths were constrained to be equal. The relative positions and areas of the Gaussians were fixed by the values shown in Table I and the only adjustable parameter was the width, which corresponds to 3.2 eV for the $L_3M_{4,5}M_{4,5}$ and 3.1 eV for the $L_2M_{4,5}M_{4,5}$ spectra. It is interesting that the $L_3M_{4,5}M_{4,5}$ widths of In, Sn, and Sb are larger and manifest considerably more dispersion.¹⁰

The agreement between theory and experiment for energies at and above that of the main peak (i.e., the "atomic" region) is quite good taking into account the fact that no attempt was made to optimize the Coulomb atomic integrals. The theoretical spectra reproduce well the shape and relative intensities of all the atomic experimental

TABLE I. Relative energies and intensities of the Ag $L_{2,3}M_{4,5}M_{4,5}$ spectra calculated in the jj IC scheme. The order of the entries in the first column corresponds to that of the bars in Figs. 1 and 2. The term indicated in column 2 is the zero spin-orbit limit of the IC state. Column 3 gives the IC relative energies in eV, whereas columns 4 and 5 present, respectively, the $L_3M_{4,5}M_{4,5}$ and $L_2M_{4,5}M_{4,5}$ intensities relative to that of the corresponding 1G_4 term.

Term	Rel. energy	L_3MM int.	L_2MM int.	
a	1S_0	-15.62	0.00	0.02
b	3P_2	-1.90	0.08	0.21
c	1G_4	0.00	1.00	1.00
d	3P_1	1.40	0.01	0.02
e	3P_0	2.39	0.04	0.02
f	1D_2	4.30	0.04	0.07
g	3F_3	8.49	0.13	0.12
h	3F_2	9.17	0.19	0.01
i	3F_4	13.72	0.29	0.03

TABLE II. Eigenvectors for Ag $4d^8$ states in intermediate coupling (J, i). The second column indicates (in parentheses) the zero spin-orbit coupling limit of state (J, i) and the corresponding line in Table I and Figs. 1 and 2.

$C_{Ji}(^{2S+1}L_J)$	Zero spin-orbit limit	Ag
$C_{01}(^1S_0)$	3P_0 (e)	-0.94
$C_{01}(^3P_0)$	3P_0 (e)	0.35
$C_{02}(^1S_0)$	1S_0 (a)	0.44
$C_{02}(^3P_0)$	1S_0 (a)	0.94
$C_{11}(^3P_1)$	3P_1 (d)	1.00
$C_{21}(^3F_2)$	3F_2 (h)	-0.59
$C_{21}(^1D_2)$	3F_2 (h)	0.68
$C_{21}(^3P_2)$	3F_2 (h)	0.44
$C_{22}(^3F_2)$	1D_2 (f)	0.67
$C_{22}(^1D_2)$	1D_2 (f)	0.11
$C_{22}(^3P_2)$	1D_2 (f)	0.73
$C_{23}(^3F_2)$	3P_2 (b)	0.45
$C_{23}(^1D_2)$	3P_2 (b)	0.73
$C_{23}(^3P_2)$	3P_2 (b)	-0.52
$C_{31}(^3F_3)$	3F_3 (g)	1.00
$C_{41}(^1G_4)$	3F_4 (i)	0.18
$C_{41}(^3F_4)$	3F_4 (i)	0.98
$C_{42}(^1G_4)$	1G_4 (c)	0.98
$C_{42}(^3F_4)$	1G_4 (c)	-0.18

peaks, as in the case of the corresponding In, Sn, and Sb spectra.¹⁰ Optimization of the Coulomb integrals would improve the agreement still further but, because of the experimental noise, such optimization was not felt to be useful. The largest disagreement in both figures is in the region between the main peak and the first to the right (i.e., region *b*), where the theoretical result is significantly less than the experimental.

In contrast to the In, Sn, and Sb spectra in I, the positions of the two peaks denominated "losses" on the low-kinetic-energy sides of the spectra in Figs. 1 and 2 (i.e., the "loss" region) do not agree with the energies of plasmon losses.^{25,26} We address the question of whether these losses are intrinsic to the Auger transition or are extrinsic by considering the Ag $L_3M_{4,5}M_{4,5}$ transition in a $Ag_{0.5}Pd_{0.5}$ alloy, shown in Fig. 3 (for convenience of notation, we denote the distance between the main peak and the minimum energy in Fig. 3 as Δ). When the raw pure Ag $L_3M_{4,5}M_{4,5}$ spectrum, scaled such that the difference between the maximum intensity and that at a distance Δ below the main peak is the same as the corresponding difference in the alloy, is subtracted from the raw spectrum in the alloy, after aligning the main peaks, we derive the result labeled $L_3(AgPd)-L_3(Ag)$ in Fig. 3. The essential vanishing of this difference spectrum indicates the invariant nature of the form of the $L_3M_{4,5}M_{4,5}$ spectrum in both the loss and atomic regions. Indeed, it would seem that whatever variation exists is greatest in the atomic region. This result, which is true of all alloys studied, combined with the absence of any influence of the Ag loss structure of any of the other XPS and XAES lines in either pure Ag or the AgPd alloys studied, as well as the absence of any sign of the corresponding Pd

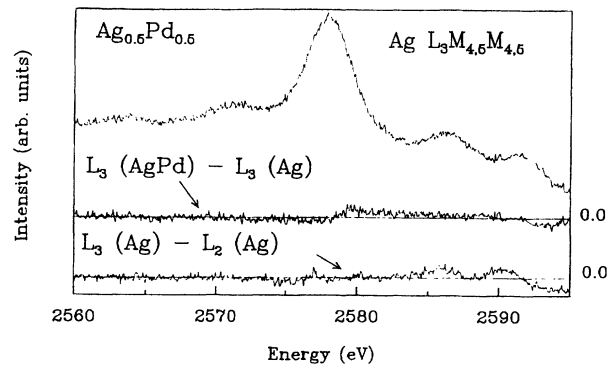


FIG. 3. The upper curve represents the Ag $L_3M_{4,5}M_{4,5}$ Auger spectra in $Ag_{0.5}Pd_{0.5}$ without background subtraction. The graph labeled $L_3(AgPd)-L_3(Ag)$ is the result of subtracting the pure Ag from the alloy $Ag_{0.5}Pd_{0.5}$ Auger spectra, after aligning the main peaks and scaling them as in Figs. 1 and 2. That denoted by $L_3(Ag)-L_2(Ag)$ corresponds to aligning the main peaks of the raw data in Figs. 1 and 2 and then subtracting. This figure indicates the similarity in the form of the loss spectra and their intrinsic nature, as discussed in the text.

$L_3M_{4,5}M_{4,5}$ losses (discussed elsewhere²⁷) in the Ag spectra, would seem to indicate that we may consider the loss structure as intrinsic to the $L_3M_{4,5}M_{4,5}$ transition.

Another interesting question concerns the relation between the $L_3M_{4,5}M_{4,5}$ and $L_2M_{4,5}M_{4,5}$ loss structures in pure Ag. In order to explore this matter, we present, in Fig. 3, the difference spectrum between the raw spectra in Figs. 1 and 2, labeled $L_3(Ag)-L_2(Ag)$, calculated in the same manner as the alloy difference spectrum discussed in the previous paragraph. The nonzero differences in the atomic region correspond to the multiplet differences. In the loss region, however, the difference spectrum essentially vanishes, indicating the remarkable similarity in the shape of the $L_3M_{4,5}M_{4,5}$ and $L_2M_{4,5}M_{4,5}$ loss structures.

An earlier study¹⁷ considered these Auger spectra of Ag, Cd, In, Sn, and Sb. The measured energies of the 1G_4 terms and the experimental spectra¹⁷ agree with our results for Ag, presented here, and for In, Sn, and Sb.¹⁰ The calculated relative term energies and intensities also agree with each other^{10,17} and with the atomic experimental peaks, even though the relative energies were calculated differently.

Analysis of the losses of the Auger spectra of these metals¹⁷ was based on associating each multiplet term of a metal with a simulated loss spectrum determined from the electron-energy-loss spectrum corresponding to energies close to that of the Auger electrons; this determination was performed by fitting Gaussian-type structures superimposed on a background to the electron-energy-loss data and by broadening the fit to obtain an elastic peak width close to that of the 1G_4 term.¹⁷ In all the metals considered, the peaks in the loss structures at energies below that of the main peak were interpreted as corresponding to plasmon satellites, in reportedly good agreement with previous measurements.²⁸⁻³⁰ Of possible satellite contributions, only those produced by the

$L_1 \rightarrow L_3 M_{4,5} \rightarrow M_{4,5} M_{4,5} M_{4,5}$ cascade were considered, and these were interpreted as relatively featureless and broad, since the loss peaks were attributed to plasmons.¹⁷

Our results for the losses of the In, Sn, and Sb Auger spectra¹⁰ are in agreement with the plasmon interpretation.¹⁷ A reasonable procedure for representing plasmon peaks is that of fitting the loss region to the sum of a polynomial background and Gaussian peaks whose energies relative to that of the 1G_4 peak are those of measured plasmons. Such a procedure fails for Ag, however. The loss peaks in Figs. 1 and 2 do not agree with measured plasmon energies,^{25,26} as we have already mentioned. The invariance of the Auger loss structure in AgPd illustrated in Fig. 3 supports this conclusion, since plasmon energies depend on environment (as reflected, for example, in the losses associated with Ag XPS spectra in the alloy) and, as we have indicated, underscores the intrinsic nature of the losses discussed above.

The agreement achieved by treating the losses as extrinsic plasmon peaks¹⁷ is difficult to understand. We should note that detailed fitting of these spectra is sensitive to the model of background employed: since the background in Ref. 17 was not described, further comment is futile (remeasurement of the electron-energy-loss spectra would be interesting, but we cannot, at present, perform this measurement). The background we use here²⁰ has the virtue of being well defined and applicable to features intrinsic to the transition. The spectral comparison in Fig. 3 involves raw data.

III. DISCUSSION

The loss features of the Ag $L_{2,3} M_{4,5} M_{4,5}$ spectra which we report here are reminiscent of those associated with the corresponding spectra of the $3d$ metals, which have been the subject of considerable attention for more than 16 years (e.g., Refs. 15 and 30–45). Examination of the similarities, as well as the differences, between the Ag and the $3d$ $L_{2,3} M_{4,5} M_{4,5}$ spectra facilitates interpretation of the former.

In particular, the satellites of the Cu $L_{2,3} M_{4,5} M_{4,5}$ Auger spectra, which have been the most studied,^{15,31,33–36,38–42} seem to arise from M spectator vacancies produced before the Auger process, although some controversy has arisen.^{40,41} The L_3 satellite seems mainly to originate in a $L_2 L_3 M_{4,5}$ Coster-Kronig (CK) transition preceding the $L_3 M_{4,5} M_{4,5}$ recombination; a substantial fraction of the initial $L_3 M_{4,5}$ states, however, seem to be produced directly in the photoemission process³⁹ (i.e., shake-up and shake-off). The L_2 satellite, on the other hand, seems to be consistently explained by the combination of an initial-state shake-up process and a $L_1 L_2 M_{4,5}$ CK transition preceding the $L_2 M_{4,5} M_{4,5}$ process.⁴²

In order to appreciate the striking character of the Ag satellites, it is well to review the salient features of their Cu counterparts: (a) both the L_3 and L_2 Cu satellites are shifted approximately the same amounts from their respective main peaks, and calculations of the relative positions based on the spectator hole model (so that the satellite corresponds to the $L_3 M_{4,5} \rightarrow M_{4,5} M_{4,5} M_{4,5}$ transition) reproduce the data quite well;³⁶ (b) the ratio of the

L_2 to the L_3 main peak is much less than that based on initial-state multiplicities—the deficit in L_2 intensity is transferred to the L_3 satellite through the $L_2 L_3 M_{4,5}$ CK process mentioned above;³⁹ (c) the double-peak structure of the L_3 satellite seems to be caused by multiplet splitting of the $3d^7$ final state;³⁶ and (d) the ratios of the satellite to main spectrum intensities of both the L_3 and L_2 spectra are about the same for photon energies below the L_1 threshold³⁸—since the CK process can be thought of as taking holes from the main L_2 line and donating them to the L_3 satellite, and since the L_2 satellite has an unusually long lifetime,^{36,39} interpretation of these satellite line shapes is complicated.

For the Ag $L_{2,3} M_{4,5} M_{4,5}$ spectra reported here, we note the following. (a) Both the L_3 and L_2 losses are displaced the same amount relative to their respective main peaks, as is especially clear in the L_3 - L_2 difference spectrum in Fig. 3; this would suggest validity of the spectator vacancy model—the most likely candidate being a $N_{4,5}$ vacancy. (b) The ratio of the L_3 and L_2 intensities is around 2.2, or very close to the statistical ratio, so that, since the losses have similar shapes, we can expect this ratio to be valid for the main (i.e., no loss) spectrum as well, this would suggest that $L_2 L_3 X$ CK processes contribute little. (c) The shape of the loss structure in Figs. 1 and 2 would not seem to be attributable to multiplet splitting of the final state with the spectator vacancy, since both losses have approximately the same shape, whereas the corresponding atomic spectra have quite different forms. Indeed, spectator vacancies consistent with the relative positions (in particular, $N_{4,5}$ vacancies) would not be expected to greatly modify the multiplet splitting of the $M_{4,5} M_{4,5}$ hole state. (d) The ratios of loss to main spectrum intensities is very similar for both the L_2 and L_3 spectra, as in the case of Cu; the apparent absence of CK processes in Ag, however, suggests the necessity of a unified explanation of both spectra. This last point serves to eliminate immediately the possibility that the $L_1 L_3 M_{4,5}$ CK process contributes significantly to the loss spectrum,¹⁷ since the $L_1 L_2 M_{4,5}$ process is forbidden in Ag.

We can estimate the relative position of a spectator vacancy-induced satellite through some simple considerations. Consider an ijk Auger transition and suppose the total energy of the metal of atomic number Z to be denoted by $E(Z; n_i, n_j, n_k, n_l)$, where the occupation number of state i is denoted by n_i , and the spectator vacancy is in state l . The Auger kinetic energy of the ijk transition, $\epsilon(Z)$, is given by Eq. (1),⁴³

$$\epsilon(Z) = E(Z; 0, 1, 1, 1) - E(Z; 1, 0, 0, 1) . \quad (1)$$

In the process involving the spectator vacancy, corresponding to the transition between hole states $il \rightarrow jkl$ (in our case $i = L_{2,3}$, and $j = k = M_{4,5}$), the kinetic energy of the satellite, $\epsilon_{\text{sat}}(Z)$, is given in Eq. (2):

$$\epsilon_{\text{sat}}(Z) = E(Z; 0, 1, 1, 0) - E(Z; 1, 0, 0, 0) . \quad (2)$$

The position of the satellite relative to that of the main peak is $\Delta\epsilon(Z) \equiv \epsilon(Z) - \epsilon_{\text{sat}}(Z)$, as in Eqs. (3),

$$\begin{aligned}\Delta\epsilon(Z) &= [E(Z; 1, 0, 0, 0) - E(Z; 1, 0, 0, 1)] \\ &\quad + [E(Z; 0, 1, 1, 1) - E(Z; 0, 1, 1, 0)] \\ &= B_l^{(j,k)}(Z) - B_l^{(i)}(Z),\end{aligned}\quad (3)$$

where we have rewritten the expressions in terms of $B_l^{(i)}(Z)$, the binding energy of state l when there is a hole in state i , and $B_l^{(j,k)}(Z)$, that of state l when there are holes in states j and k .⁴³ Applying the excited-atom model,⁴⁴ we can treat the core holes as extra protons, which results in Eq. (4),

$$\Delta\epsilon(Z) \simeq B_l(Z+2) - B_l(Z+1). \quad (4)$$

The binding energy can be separated into contributions originating with the valence and the core states.^{7,11,13} From the point of view of the valence electrons, treating the j and k core holes in Eq. (3) as extra protons is certainly a good approximation.^{3,7,11,13} Whether this approximation is valid for the core contribution really depends on the relative spatial extent of the j and k core holes and the l state. Although we expect Eq. (4) to be, in general, at least a rough approximation to $\Delta\epsilon(Z)$, its accuracy should improve as the l state becomes more diffuse. For example, for $l = N_{4,5}$, a valence d -band state, Eq. (4) may constitute a quite reasonable approximation of $\Delta\epsilon(Z)$.

In the case of Ag, we can see immediately from Eq. (4) and Figs. 1 and 2 that the only spectator vacancy state that could possibly produce the losses closest to the main peak is that corresponding to a $N_{4,5}$ hole.^{45,46} All other states result in values of $\Delta\epsilon(\text{Ag})$ which are much too large.²³ Appropriate values of the experimental $N_{4,5}$ binding energies^{45,46} of Cd and In yield $\Delta\epsilon(\text{Ag}) \simeq 6.05$ eV, which is clearly close to the separations in Figs. 1 and 2. We compare this result further with experimentally derived values in our analysis of the line shapes below.

Since the loss structures in Figs. 1 and 2 appear to present two peaks, it is interesting to examine whether the loss peak farther from the main peak is also consistent with a spectator vacancy picture—in this case a double spectator vacancy.³⁷ In this case, the hole state transition would be $ilm \rightarrow jklm$ (in our case, $i = L_{2,3}$, and $j = k = M_{4,5}$). The two-hole satellite kinetic energy $\epsilon_{2\text{sat}}(Z)$ corresponds to Eq. (5), where the total energy is $E(Z; n_i, n_j, n_k, n_l, n_m)$, so that

$$\epsilon_{2\text{sat}}(Z) = E(Z; 0, 1, 1, 0, 0) - E(Z; 1, 0, 0, 0, 0). \quad (5)$$

The separation between the single and double spectator hole satellites is $\Delta\epsilon_2(Z) \equiv \epsilon_{\text{sat}}(Z) - \epsilon_{2\text{sat}}(Z)$, which we can write in terms of binding energies as in Eq. (6),

$$\Delta\epsilon_2(Z) = B_m^{(jkl)}(Z) - B_m^{(il)}(Z), \quad (6)$$

where we use the same notation as in our derivation of Eq. (3). Again treating the i , j , and k core holes as extra protons, we obtain Eq. (7):

$$\Delta\epsilon_2(Z) \simeq B_m^{(l)}(Z+2) - B_m^{(l)}(Z+1). \quad (7)$$

The binding energies in Eq. (7) can be derived from the definition of the experimental Auger parameter, ξ_{lm} ,⁴³

where we write explicitly the fact that ξ depends only on the final hole states,¹⁴

$$\xi_{lm}(Z) = B_m^{(l)}(Z) - B_m(Z). \quad (8)$$

The final approximation for $\Delta\epsilon_2(Z)$ is written in terms of experimentally measured quantities in Eq. (9),

$$\begin{aligned}\Delta\epsilon_2(Z) &\simeq B_m(Z+2) - B_m(Z+1) \\ &\quad + \xi_{lm}(Z+2) - \xi_{lm}(Z+1),\end{aligned}\quad (9)$$

where the same comments as those following Eq. (4) are applicable. Assuming the spectator holes to be in the $4d$ band (i.e., $l = m = N_{4,5}$) and using experimental quantities^{45,46} for Ag, we derive $\Delta\epsilon_2(\text{Ag}) \simeq (6.05 + 0.6)$ eV. The total separation between the main peak and the second loss peak is $\Delta\epsilon_2(\text{Ag}) + \Delta\epsilon(\text{Ag}) \simeq (6.65 + 6.05)$ eV = 12.70 eV, which, again, is in reasonable agreement with the apparent separation.

In order to verify the picture that the losses in Figs. 1 and 2 are satellites resulting from $N_{4,5}$ spectator holes, we should be able to show that the line shapes resulting from this picture are consistent with the data. In the case of Cu, the $M_{4,5}$ spectator hole produces a d^7s final state, whose multiplet splitting, as manifested in optical data,⁴⁷ is large, because of the strong spin-orbit interaction of the three $M_{4,5}$ final-state holes. The proposed $N_{4,5}$ spectator holes in Ag, however, would interact only weakly with the $M_{4,5}$ core holes because of the different atomic shells involved. The multiplet splitting resulting from the interaction of the three holes, therefore, would be little interaction different from that of the two $M_{4,5}$ holes: the major difference would appear as intrinsic broadening which results partly from the relatively slight extra multiplet splitting produced by the $N_{4,5}$ hole and partly from the width of the $4d$ band, which governs the number of possible $N_{4,5}$ hole states. In other words, we expect the satellite line shapes to be essentially broadened images of the main, atomic spectra shown in Figs. 1 and 2.

In Figs. 4 and 5, we illustrate, for the $L_3M_{4,5}M_{4,5}$ and $L_2M_{4,5}M_{4,5}$ spectra, respectively, the results of assuming that the experimental spectra result from a main atomic spectrum plus two satellite images. The component spectra are indicated by light lines and the envelope by a heavy line. The parameters resulting from fitting this picture to the data are presented in Table III for the atomic and two satellite components of the envelope. Within each component, the relative positions and intensities of the multiplet terms are given by the values in Table I corresponding to the same initial state. A component spectrum is generated by multiplying each of its terms by a Gaussian of constant amplitude and width centered at the term position. The agreement in Table III between the relative intensities and widths of the respective L_3 and L_2 components is a reflection of the loss-structure similarity illustrated in Fig. 3. We also indicate, in Table III, the results of the estimates of the relative satellite positions in Eqs. (4) and (9). Considering the simplicity of the model, the agreement is encouraging, and certainly serves to eliminate any other possible spectator vacancy as candidate. Similar agreement is

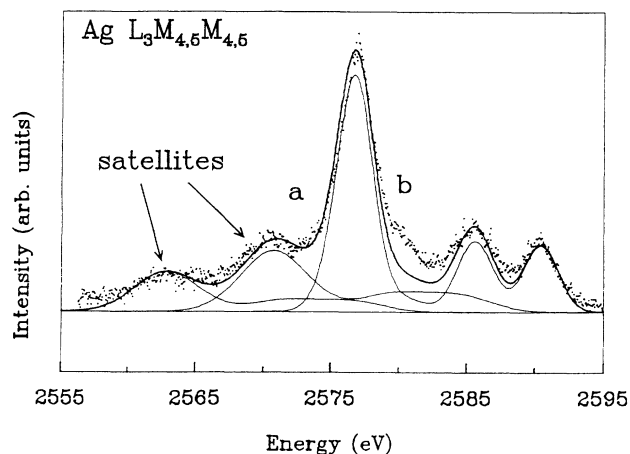


FIG. 4. The $L_3M_{4.5}M_{4.5}$ Auger spectrum of Ag with the background subtracted. The light solid curves correspond to the atomic satellite image spectra, as discussed in the text, while the heavy line is their envelope. Each of the components of the envelope corresponds to the parameters in Table I. The relation among them is given in Table III. The multiplet structure of the image spectra is necessary to achieve the agreement in region *a* as well as the improvement in agreement in region *b* with respect to Fig. 1.

achieved in analysis of the corresponding Pd and Rh spectra.²⁷

From Figs. 4 and 5, it is clear that this model is consistent with the experimental spectra: the loss region is represented well and the agreement in region *b* in Figs. 4 and 5 is improved over that shown in Figs. 1 and 2 because of contributions from the satellite images; it should also be noted that the agreement in region *a* in Figs. 4 and 5 is not achievable with a superposition of simple Gaussians centered at the satellite positions. Although this agreement does not provide unambiguous confirmation of the model (e.g., a large portion of the loss regions in Figs. 4 and 5 can be reasonably well represent-

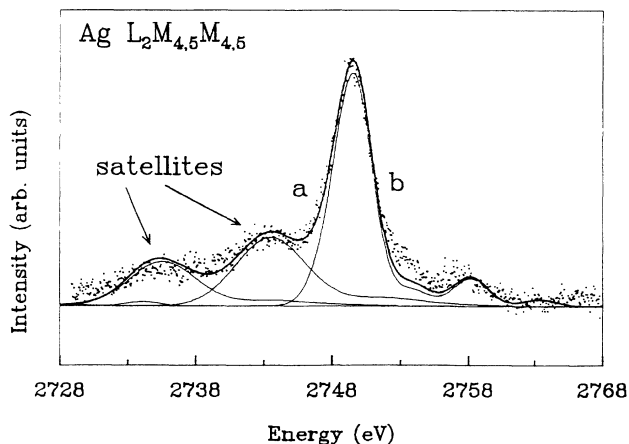


FIG. 5. The $L_2M_{4.5}M_{4.5}$ Auger spectrum of Ag with background subtracted. The same conventions as in Fig. 4 are followed here.

TABLE III. Parameters used in constructing the component spectra in Figs. 4 and 5. The second column presents the position of the 1G_4 component relative to that of the atomic theoretical spectrum. The third column represents the results of the estimates of the relative position in Eqs. (4) and (9). The multiplet splittings of the satellite spectra are the same as those of the respective atomic spectrum and are given in Table I. In each figure, each multiplet term is multiplied by a Gaussian of form $D \exp\{-[(E - E_i)/\Gamma]^2\}$, where E_i denotes the term energy, and the amplitude D and half width Γ are the same for all terms in a multiplet; the fourth column represents 2Γ . The quantity $L_i \text{ Int.}$ ($i = 3$ or 2) in the last two columns denotes the intensity relative to that of the atomic part, and is equal to $D\Gamma\sqrt{\pi}$.

	1G_4 (eV)	Est. (eV)	2Γ (eV)	$L_3 \text{ Int.}$	$L_2 \text{ Int.}$
Atomic	0.0	0.0	3.6	1.0	1.0
Satellite 2	-5.95	-6.05	6.7	0.45	0.50
Satellite 1	-13.90	-12.70	6.4	0.28	0.31

ed by the sum of two Gaussian loss peaks), the consistency of the model with *all* the aspects of the data considered in points (a)–(d) above is encouraging.

From the considerations presented here, it appears that L_2L_3X CK processes contribute little to the Ag spectra, in contrast with the situation in Cu, for example. The $N_{4.5}$ spectator holes, which, we suggest, produce the loss structure, could arise from either shake-up or $L_1L_{2,3}N_{4.5}$ CK processes;⁴⁸ since, however, $L_2L_3N_{4.5}$ CK transitions do not appear to contribute and since theoretical transition probabilities of the $L_1L_{2,3}N_{4.5}$ and $L_2L_3N_{4.5}$ are of the same order of magnitude,²⁴ it is reasonable to discard the CK processes as possible causes of the spectator holes. In fact, the data seem to oblige us to interpret the loss features of the Ag $L_{2,3}M_{4.5}M_{4.5}$ spectra as arising from shake-up satellites arising from *d*-band valence holes. Loss structure resulting from incomplete relaxation of the photoexcited state were observed previously in plasmon gain satellites of the *KLL* spectra of Na and Mg (Ref. 49) and shake-up satellites of the *KLV* spectra of Mg (Ref. 50) and Al;⁵¹ our treatment of the satellite images in Figs. 4 and 5 is similar to that of the *KLV* satellites.^{50,51}

One expects the probability of shake-up processes in photoemission to increase with increasing photon energy.⁴⁹ Since we use bremsstrahlung as the exciting radiation, the high photon energies involved may explain why shake-up processes are strong in Ag; of course, this requires that the *d*-band spectator holes be sufficiently long lived to survive until the Auger decay occurs.³ What is not clear at present is why the L_2L_3X CK processes are so weak. It should be noted that, from rough measurements of experimental peak areas, the ratios of the $L_{2,3}M_{4.5}M_{4.5}$ to $L_1M_{4.5}M_{4.5}$ intensities deviate from that of the initial-state multiplicities (i.e., $L_2/L_1 \approx 4$) so that there appear to be $L_1L_{2,3}X$ CK processes involved. The observed ratios of L_3 and L_2 intensities indicate, however, that these CK process must have approximately equal probability for both the L_3 and L_2 spectra.

IV. CONCLUSIONS

We report measurements of the $L_{2,3}M_{4,5}M_{4,5}$ spectra of Ag. The atomic portion of the spectra agree with intermediate coupling calculations of multiplet splitting and relative intensities. The loss structures observed seem to be intrinsic and not attributable to plasmon losses. The features of the data are consistent with a model in which d -band spectator holes are responsible for the loss structure. L_2L_3X Coster-Kronig processes do

not appear to be involved to any significant extent. Evidence of such unambiguous shake-up satellites has not been reported before in Auger spectra transition metals.

ACKNOWLEDGMENTS

We would like to thank R. C. G. Vinhas and R. F. Suarez for technical assistance. This work was supported by CNPq, FAPESP, and FINEP of Brazil.

- ¹B. Johansson and N. Mårtensson, *Phys. Rev. B* **21**, 4427 (1980).
²N. D. Lang and A. R. Williams, *Phys. Rev. B* **16**, 2408 (1977).
³G. G. Kleiman, *Appl. Surf. Sci.* **11/12**, 730 (1982).
⁴G. G. Kleiman, S. G. C. de Castro, J. D. Rogers, and V. S. Sundaram, *Solid State Commun.* **43**, 257 (1982).
⁵G. G. Kleiman, R. Landers, S. G. C. de Castro, and P. A. P. Nascente, *Phys. Rev. B* **45**, 13 899 (1992); *Surf. Sci.* **287/288**, 794 (1993).
⁶G. G. Kleiman, *J. Phys. Condens. Matter* **5**, 1 (1993).
⁷G. G. Kleiman, R. Landers, S. G. C. de Castro, and J. D. Rogers, *Phys. Rev. B* **44**, 8529 (1991).
⁸T. D. Thomas and P. Weightman, *Phys. Rev. B* **33**, 5406 (1986).
⁹P. A. P. Nascente, S. G. C. de Castro, R. Landers, and G. G. Kleiman, *Phys. Rev. B* **43**, 4659 (1991).
¹⁰G. G. Kleiman, R. Landers, P. A. P. Nascente, and S. G. C. de Castro, *Phys. Rev. B* **46**, 1970 (1992).
¹¹G. G. Kleiman, R. Landers, S. G. C. de Castro, and P. A. P. Nascente, *Phys. Rev. B* **44**, 3383 (1991).
¹²G. G. Kleiman, R. Landers, S. G. C. de Castro, and P. A. P. Nascente, *J. Vac. Sci. Technol. A* **10**, 2839 (1992).
¹³G. G. Kleiman, R. Landers, P. A. P. Nascente, and S. G. C. de Castro, *Phys. Rev. B* **46**, 4405 (1992); *Surf. Sci.* **287/288**, 798 (1993).
¹⁴R. Landers, P. A. P. Nascente, S. G. C. de Castro, and G. G. Kleiman, *J. Phys. Condens. Matter* **4**, 5881 (1992); *Surf. Sci.* **287/288**, 802 (1993).
¹⁵E. Antonides, E. C. Janse, and G. A. Sawatzky, *Phys. Rev. B* **15**, 1669 (1977).
¹⁶J. F. McGilp, P. Weightman, and E. J. McGuire, *J. Phys. C* **10**, 3445 (1977).
¹⁷J.-M. Mariot and M. Ohno, *Phys. Rev. B* **34**, 2182 (1986).
¹⁸C. D. Wagner and J. A. Taylor, *J. Electron Spectrosc.* **20**, 83 (1980).
¹⁹V. S. Sundaram, J. D. Rogers, and R. Landers, *J. Vac. Sci. Technol. A* **19**, 117 (1981).
²⁰D. A. Shirley, *Phys. Rev. B* **5**, 4709 (1972).
²¹E. U. Condon and G. H. Shortley, *The Theory of Atomic Spectra* (Cambridge University Press, London, 1963).
²²J. B. Mann (unpublished).
²³R. Nyholm and N. Mårtensson, *J. Phys. C* **13**, L279 (1980).
²⁴E. J. McGuire (unpublished).
²⁵A. C. Parry-Jones, P. Weightman, and P. T. Andrews, *J. Phys. C* **12**, 1587 (1979).
²⁶R. A. Pollak, L. Ley, F. R. McFeely, S. P. Kowalczyk, and D. A. Shirley, *J. Electron Spectrosc.* **3**, 381 (1974).
²⁷R. Landers, S. G. C. de Castro, and G. G. Kleiman (unpublished).
²⁸C. J. Powell, *Proc. Phys. Soc. (London)* **76**, 593 (1960).
²⁹J. Robins, *Proc. Phys. Soc. (London)* **78**, 1177 (1961).
³⁰J. L. Robins, *Proc. Phys. Soc. (London)* **79**, 119 (1962).
³¹E. D. Roberts, P. Weightman, and C. E. Johnson, *J. Phys. C* **8**, L301 (1975).
³²E. Antonides and G. A. Sawatzky, *J. Phys. C* **9**, L547 (1976).
³³E. Antonides, E. C. Janse, and G. A. Sawatzky, *Phys. Rev. B* **15**, 4596 (1977).
³⁴H. W. Haak, G. A. Sawatzky, and T. D. Thomas, *Phys. Rev. Lett.* **41**, 1825 (1978).
³⁵P. Weightman and P. T. Andrews, *J. Phys. C* **12**, 943 (1979).
³⁶N. Mårtensson and B. Johansson, *Phys. Rev. B* **28**, 3733 (1983).
³⁷N. Mårtensson, R. Nyholm, and B. Johansson, *Phys. Rev. B* **30**, 2245 (1984).
³⁸D. D. Sarma, C. Carbone, P. Sen, R. Cimino, and W. Gudat, *Phys. Rev. Lett.* **63**, 656 (1989).
³⁹N. Wassdahl, J.-E. Rubensson, G. Bray, P. Glans, P. Bleckert, R. Nyholm, S. Cramm, N. Mårtensson, and J. Nordgren, *Phys. Rev. Lett.* **64**, 2807 (1990).
⁴⁰J. C. Fuggle and G. A. Sawatzky, *Phys. Rev. Lett.* **66**, 966 (1991).
⁴¹D. D. Sarma, C. Carbone, P. Sen, R. Cimino, and W. Gudat, *Phys. Rev. Lett.* **66**, 967 (1991).
⁴²S. M. Thurgate and J. Neale, *Surf. Sci. Lett.* **256**, L605 (1991).
⁴³N. D. Lang and A. R. Williams, *Phys. Rev. B* **20**, 1369 (1979).
⁴⁴A. R. Williams and N. D. Lang, *Phys. Rev. Lett.* **40**, 954 (1978).
⁴⁵N. Mårtensson and R. Nyholm, *Phys. Rev. B* **24**, 7121 (1981).
⁴⁶We have taken the binding energy of the $N_{4,5}$ as equal to $\frac{1}{2}$ the uncorrelated experimental double hole binding energy from Ref. 45.
⁴⁷C. E. Moore, *Atomic Energy Levels*, Natl. Bur. Stand. (U.S.) Circ. No. 467 (U.S. GPO, Washington, D.C., 1958), Vol. II.
⁴⁸D. E. Ramaker (private communication).
⁴⁹J. C. Fuggle, R. Lässer, O. Gunnarsson, and K. Schönhammer, *Phys. Rev. Lett.* **44**, 1090 (1980).
⁵⁰M. Davies, D. R. Jennison, and P. Weightman, *J. Phys. C* **17**, L107 (1984).
⁵¹P. H. Hannah and P. Weightman, *J. Phys. C* **18**, L239 (1985).